Adsorption (2015) 21:499–507
DOI 10.1007/s10450-015-9688-2

Seeking metal–organic frameworks for methane storage in natural gas vehicles

Jia Fu[1] · Yun Tian[1] · Jianzhong Wu[1]

Received: 17 December 2014 / Revised: 20 July 2015 / Accepted: 10 September 2015 / Published online: 16 September 2015

Abstract Promising metal–organic frameworks (MOFs) have been identified from Grand Canonical Monte Carlo simulation to meet the ARPA-E target for methane storage in natural gas vehicles set by the U.S. Department of Energy (DOE). While none of MOF materials known today are able to meet the ARPA-E target for in vehicle natural gas storage, it could be reached by relaxing the operation conditions for gas compression and delivery. When methane is compressed at 298 K and 170 bar and released at 358 K and 5 bar, top ranked MOFs are able to deliver over 90 % of the required gas delivery amount. Besides, a large number of MOF materials could achieve the ARPA-E target 100 % if the compression temperature is set to 233 K. The simulation results provide useful insights into chemical and geometric characteristics of new materials for methane storage. Future materials development should be focused on improving the volumetric delivery amount rather than the total volumetric gas storage capacity that is often quoted in the literature.

Graphical Abstract Monte Carlo simulation identifies promising MOF materials and operation parameters to meet the ARPA-E target for methane storage.

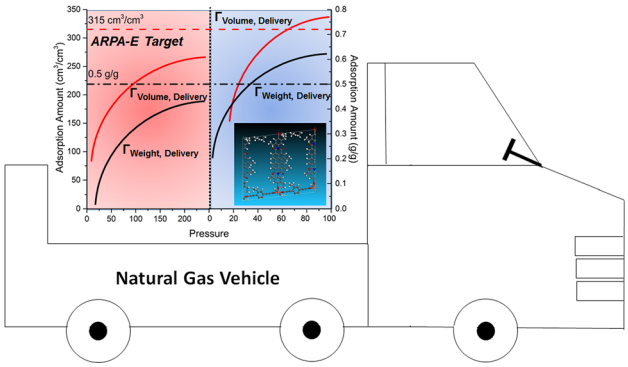

Keywords Monte Carlo simulation · ARPA-E target · Methane storage · MOF

1 Introduction

Concerns over the national energy security and global climate changes are calling for the development of alternative transportation fuels that have minimal carbon footprint yet reliable supplies. The low cost and huge reserve of natural gas (NG) discovered in recent years make it an attractive choice. NG is mainly composed of methane that has a high research octane number (RON = 107) and contributes no SO_x and NO_x emissions (Lozano-Castelló et al. 2002). While the performance of natural gas vehicles (NGV) is almost comparable with those of equivalent conventional vehicles, one of the key challenges in their broader use lies in the storage and delivery of a large amount of gas at ambient conditions. At present, NGVs employ heavy-duty tanks containing either liquefied natural gas (LNG) or compressed natural gas (CNG) (He et al. 2014). The gas storage involves cryogenic (112 K) and

Electronic supplementary material The online version of this article (doi:10.1007/s10450-015-9688-2) contains supplementary material, which is available to authorized users.

✉ Jianzhong Wu
jwu@engr.ucr.edu

[1] Department of Chemical and Environmental Engineering, University of California, Riverside, CA 92521, USA

high-pressure (>200 bar) operations that are too expensive, energetically inefficient, and hazardous for many practical applications. Recent years have witnessed tremendous developments in Adsorbed Natural Gas (ANG) based on activated carbons or nanostructured porous materials such as metal–organic frameworks (MOFs) (Li et al. 2014b). ANG is promising for NGV applications owing to its excellent gas storage capability at relatively moderate conditions (Celzard and Fierro 2005; Chui et al. 1999; Düren et al. 2004; He et al. 2014; Liu et al. 2012; Ma et al. 2008; Makal et al. 2012; Mason et al. 2014; Peng et al. 2013a; Rosi et al. 2003; Suh et al. 2011; Sumida et al. 2011).

Unlike amorphous porous materials such as activated carbons, MOFs have predicable crystalline structures and diverse modular building blocks (Eddaoudi et al. 2001, 2002a, b; Yaghi et al. 2003). These materials can be synthesized at the industrial scale. [e.g., BASF(BASF)] A wide variety of MOFs have been reported potentially useful for CH_4 storage. Prominent examples include HKUST-1, (Peng et al. 2013a) MOF-5, (Mason et al. 2014) NU-111, (Peng et al. 2013b) NU-125, (Wilmer et al. 2013) NU-800, (Gomez-Gualdron et al. 2014) UTSA-20, (Guo et al. 2011) UTSA-76, (Li et al. 2014a) PCN-14, (Ma et al. 2007) NiMOF-74 (Wu et al. 2009). Recently, Yaghi's group demonstrated that MOF-519 (Gándara et al. 2014) provides an impressive methane delivery amount of 230 cm^3/cm^3 at 298 K for compression and release at 80 and 5 bar, respectively. While that capacity is higher than any MOFs presently known, it does not yet meet the ARPA-E target (Wilmer et al. 2013). Under the same operating conditions, the ARPA-E goal for methane storage demands a volumetric delivery amount above 315 cm^3(STP)/cm^3 (corresponding to energy density 12.5 MJ/L, the same as CNG at 250 bar and 298 K) and a weight delivery amount above 0.5 g/g.

The number of MOFs that have been tested for methane storage is trivially small in comparison to the huge variety of the nanostructures that could be synthesized. Because experimental studies for a large number of materials are tedious and time consuming, computational methods such as the classical molecular simulation are a welcome choice in the materials community (Düren et al. 2004; Frost et al. 2006; Garberoglio et al. 2005; Liu and Smit 2010; Skoulidas and Sholl 2005; Walton and Snurr 2007; Yang and Zhong 2006). For example, Wilmer et al. (2012) and Gómez-Gualdrón et al. (2014) used grand canonical Monte Carlo (GCMC) simulation to predict methane adsorption in about 100,000 hypothetical MOFs and identified a small group for tailored synthesis. Martin et al. (2014) utilized commercially available chemical fragments with experimentally known synthetic routes to design 18,000 synthetically realistic Porous Polymer Networks (PPNs) by computational methods. Important geometric and chemical characteristics of PNPs were identified for methane storage. It was found that cooperative methane–methane attractions must be considered for optimal materials design. Recently, Gómez-Gualdrón et al. (2014) explored the limits of nanoporous materials for methane storage and delivery. They concluded that none of the existing MOFs meet the ARPA-E target, at least for gas storage at ambient temperature (298 K) and moderate pressure (<65 bar). Nevertheless, the simulation studies suggest that alkyne groups are more favorable than phenyl rings for gas storage due to more efficient packing around the binding sites (Gomez-Gualdron et al. 2014). By screening over 200 hypothetical MOFs based on zirconium inorgianc nodes, GCMC simulation helps the successful design and synthesis of NU-800, a new stable MOF with a methane deliverable capacity of 167 cm^3/cm^3 at the ARPA-E operation conditions. Rana et al. (2014) studied the adsorption thermodynamics, electronic structure and methane storage capacity of a series of metal substituted *M*-2,5-oxidobenzene-1,4-dicarboxylate and other prominent MOFs. Significant gaps were identified between the total and usable capacities of these materials for both isothermal pressure swing (PS) and temperature plus pressure swing (TPS) processes. It was found that optimal methane adsorbents should maximize the capacity while minimizing the thermal loads.

In this work, we use GCMC to identify promising MOFs for NGV applications and explore possible alternatives to reach the ARPA-E target by changing the operation conditions for gas compression and delivery. In addition, we examine the chemical and geometric characteristics of the promising MOFs and highlight important indicators for future material developments.

2 Methods

We use the grand canonical Monte Carlo (GCMC) simulation to study methane adsorption in various metal–organic frameworks (MOFs) (Frenkel and Smit 2001). The fluid-framework and fluid–fluid interactions are modeled by the Lennard-Jones (LJ) 12-6 potential:

$$u_{ij}(r) = 4\varepsilon_{ij}\left[\left(\frac{\sigma_{ij}}{r}\right)^{12} - \left(\frac{\sigma_{ij}}{r}\right)^{6}\right] \quad (1)$$

where σ and ε are the LJ size and energy parameters, respectively. As in a standard force field, the Lorentz–Berthelot (LB) mixing rule is employed for different atom types. The LJ parameters for MOFs are taken from the UFF force field (Rappe et al. 1992). It has been shown that, in general, UFF is accurate for predicting gas adsorption in MOFs at room temperature (Düren et al. 2004; Rana et al.

2014). For CH_4 molecules, the LJ parameters are obtained from TraPPE force field ($\varepsilon_{CH4}/k_B = 148.0$ K and $\sigma_{CH4} = 3.73$ Å). These parameters are able to reproduce the methane critical temperature and saturated liquid densities (Martin and Siepmann, 1998).

As a general rule for selecting the simulation box, we use a $2 \times 2 \times 2$ supercell of the unit crystalline structure for each MOF framework. GCMC simulations are performed with the conventional three dimensional periodic boundary conditions (PBC). The van der Waals interactions were evaluated with a spherical cutoff of 12.9 Å. For most MOFs considered in this work, the supercell ensures that the simulation box is larger than twice of the cut-off distance in each dimension. For MOFs with very small unit cells, we increase the supercell size by adding more repeating unit cells of the crystalline structure to make sure that each dimension is larger than twice of the cut-off distance. As in typical GCMC simulations, we use 10^6 trial moves to reach the equilibrium state, and subsequent 10^6 moves for calculating ensemble averages. The chemical potential for methane gas is calculated from the MBWR equation of state (Johnson et al. 1993). The data from each simulation trajectory is divided into ten blocks in order to estimate statistical uncertainties. Unless specifically mentioned, the statistical uncertainty is generally smaller than the symbol sizes presented in the figures. All GCMC simulations are carried out with the Towhee 7.0.4 program (Martin 2013).

3 Results

We consider over 1000 MOF candidates from the Northwestern Hypothetical MOF Database that were previously identified by different characteristic properties at 298 K and 35 bar (Wilmer et al. 2012). These materials are chosen from the top rankings according to four different criteria: (1) top 300 MOFs based on the excess CH_4 adsorption per material weight (weight category); (2) top 300 MOFs based on the excess CH_4 adsorption per material volume (volume category); (3) top 300 MOFs based on the material void fraction (void fraction category); and (4) top 300 MOFs based on the material specific surface area (m^2/cm^3) (surface area category). In selection of these materials, we remove the duplicates such that each material appears only in one of the four categories.

As in a previous work (Fu et al. 2015), we start with GCMC calculations for methane adsorption at 298 K and 35 bar and release at the same temperature but at 5 bar. These operation conditions are the same as those specified in the ARPA-E target. Figure 1 shows our GCMC predictions for both the total and the deliverable capacities (between compression at 298 K and 35 bar and release at the same temperature and 5 bar). For those top MOFs in the volume category (see Fig. 1a, c), the GCMC results indicate that, even in terms of the total storage capacity at 298 K and 35 bar, none of these materials meet the ARPA-E target of 260 cm^3(STP)/cm^3 (with an energy density of 9.2 MJ/L, corresponding to that of CNG at 250 bar without considering 25 % packing loss). Ironically, MOFs with high total volumetric adsorption often have small deliverable capacity, typically less than 20 % of the total uptake at 35 bar.

Top MOF materials in the volume category are characterized by large specific surface area and favorable surface interactions. Due to the strong attraction of these materials with CH_4 molecules, a large amount of adsorbed gas persists at low pressure. As indicated by Rana et al. (2014), the total adsorption capacity is not a good indicator to evaluate MOFs for NGV applications. Modifications to enhance methane attraction at the binding sites (such as unsaturated metal nodes) are also not recommended due to strong adsorption at low pressure. As a result, we expect that materials with moderate interaction with methane molecules are most likely to have high delivery amount. Our simulation results show no clear correlation between the weight adsorption capacity and the total volumetric storage (see also Tables S1-S10 in Support Information (SI)).

Figure 1c shows that MOFs with the highest volumetric delivery capacity may also have a large weight adsorption capacity, even though the total volumetric capacity is not necessarily ranked on the top. In terms of the gravimetric adsorption amount (Fig. 1b, d), the total and delivery capacities follow similar trends. In particular, MOF (5003) has the highest total gas weight uptake and the best delivery capacity. The top candidates in the weight category rank poorly in terms of the volumetric adsorption, less than 40 % in comparison to the top-ranked MOFs shown in Fig. 1a, c. Surprisingly, those top candidates have very close total and delivery amounts in the volumetric category. It appears that those materials do not have many favorable binding sites, acting as if gas molecules were in a usual compressed tank. Considering all possible measures, we find that the volumetric deliverable amount is probably the most important criterion to select MOF materials for NGV applications. A similar conclusion was reached from recent experimental studies of the NGV driving range (Mason et al. 2014). In the following discussions, we thus focus on materials performance in terms of the volumetric deliverable capacity.

We may boost the volumetric delivery amount either by increasing the gas uptake at the compression stage or by reducing the remnant amount upon release. Figure 2 shows the performance of some top ranked MOFs from the volume category if we set the initial pressure higher than

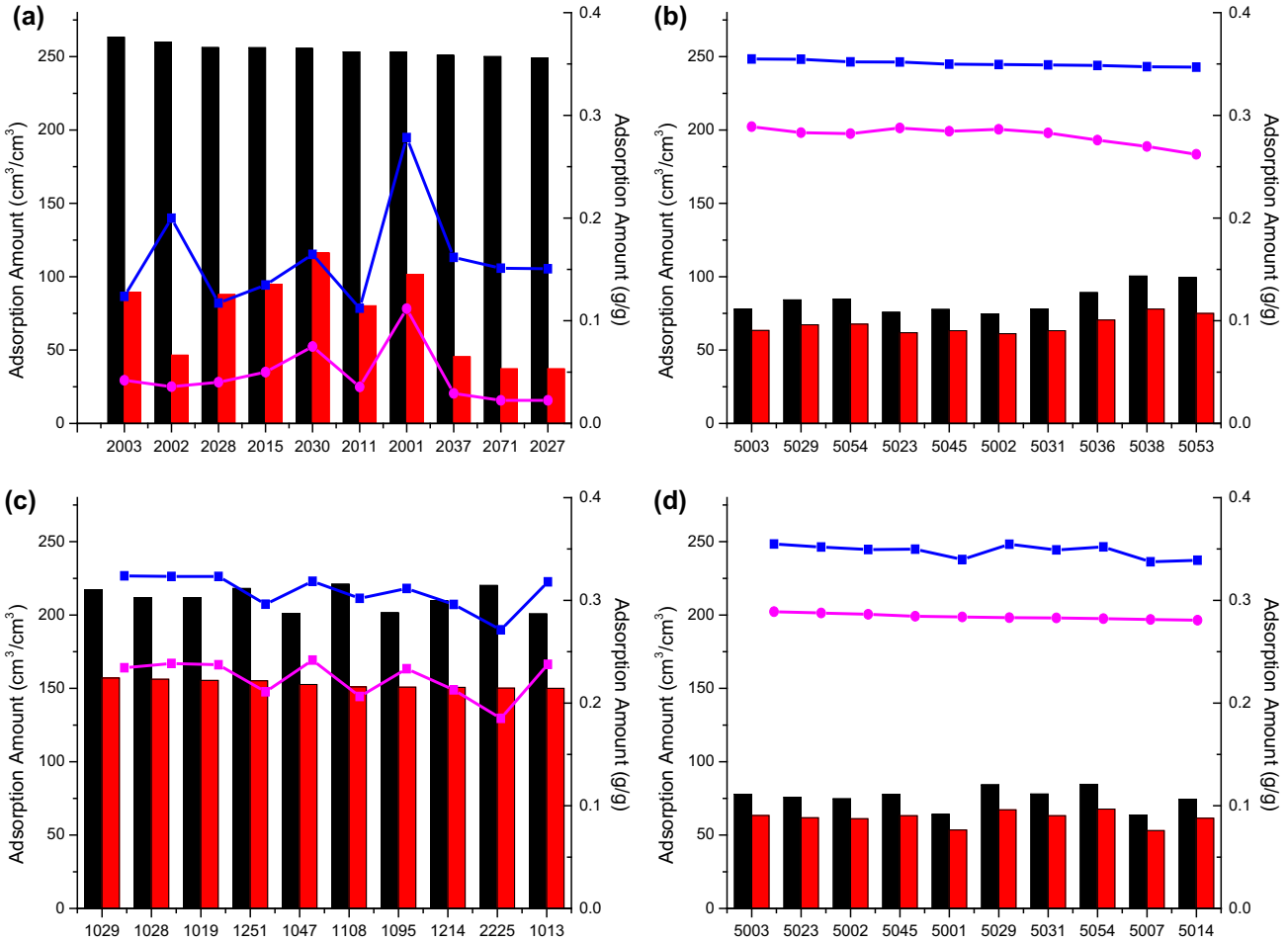

Fig. 1 Top ten MOF materials identifed from simulation accordingly to their performance at 298 K and 35 bar in terms of **a** total volumetric adsorption; **b** total weight adsorption; **c** volumetric delivery amount (released at the same temperature and 5 bar); **d** Weight delivery amount. In *each panel*, the horizontal axis gives the serial numbers in the Northwestern Hypothetical MOF Database (Wilmer et al. 2012); the 1st digit represents the category of ranking, i.e., one for excess CH_4 adsorption in the weight category; two for excess CH_4 adsorption in the volume category; and five for the void fraction category. The last three digits of each serial number denote the ranking within the individual category. Here *black* and *red column bars* stand for the total and delivery volumetric adsorption amounts, *blue* and *pink lines* correspond to the total and delivery weight adsorption amounts, respectively (Color figure online)

35 bar. More extensive results are given in Tables S11-S20. Figure 2a shows that both the volumetric and weight deliverable amounts increase by nearly 30 % if we double the compression pressure (i.e., from 35 to 70 bar). However, the delivery capacity reaches only up to about 60 % of the ARPA-E target, even for the top ranked MOF materials. The volumetric target [i.e., 260 cm^3(STP)/cm^3] could be reached only if the pressure is further increased to 170 bar. While the volumetric target appears unattainable [i.e., 315 cm^3(STP)/cm^3], the weight deliverable amount has already exceeded the 0.5 g/g target, suggesting that 170 bar could be taken as the upper limit for studying the adsorbed methane storage capacity at room temperature. At this pressure, most MOFs approach the saturation limit of their CH_4 storage capacity, i.e., a further increase of the compression pressure does not have much effect on the volumetric delivery amount.

Figure 2c shows that, when the compression pressure is further increased to 250 bar, the same as that in the CNG gas tank, the total adsorption amount is 50 % higher than that at 170 bar (Fig. 2b). However, we only increase the volumetric delivery amount less than 5 %. Gómez-Gualdrón et al. (2014) and Wilmer et al. (2012) suggested that MOF materials could reach the ARPA-E target only if the attractive energy between the gas and substrate is quadrupled and if the release temperature is increased to 398 K.

Considering that the tolerated temperate range for CH_4 operation is between −40 and 85 °C in the ARPA-E project (ARPA-E 2015), we have also investigated the effect of the two temperature boundaries on methane adsorption. In one case, we raise the adsorption amount by lowering the compression temperature to 233 K. In another case, we increase the delivery temperature to 358 K so that the remnant gas adsorption could be minimized. Figure 2d

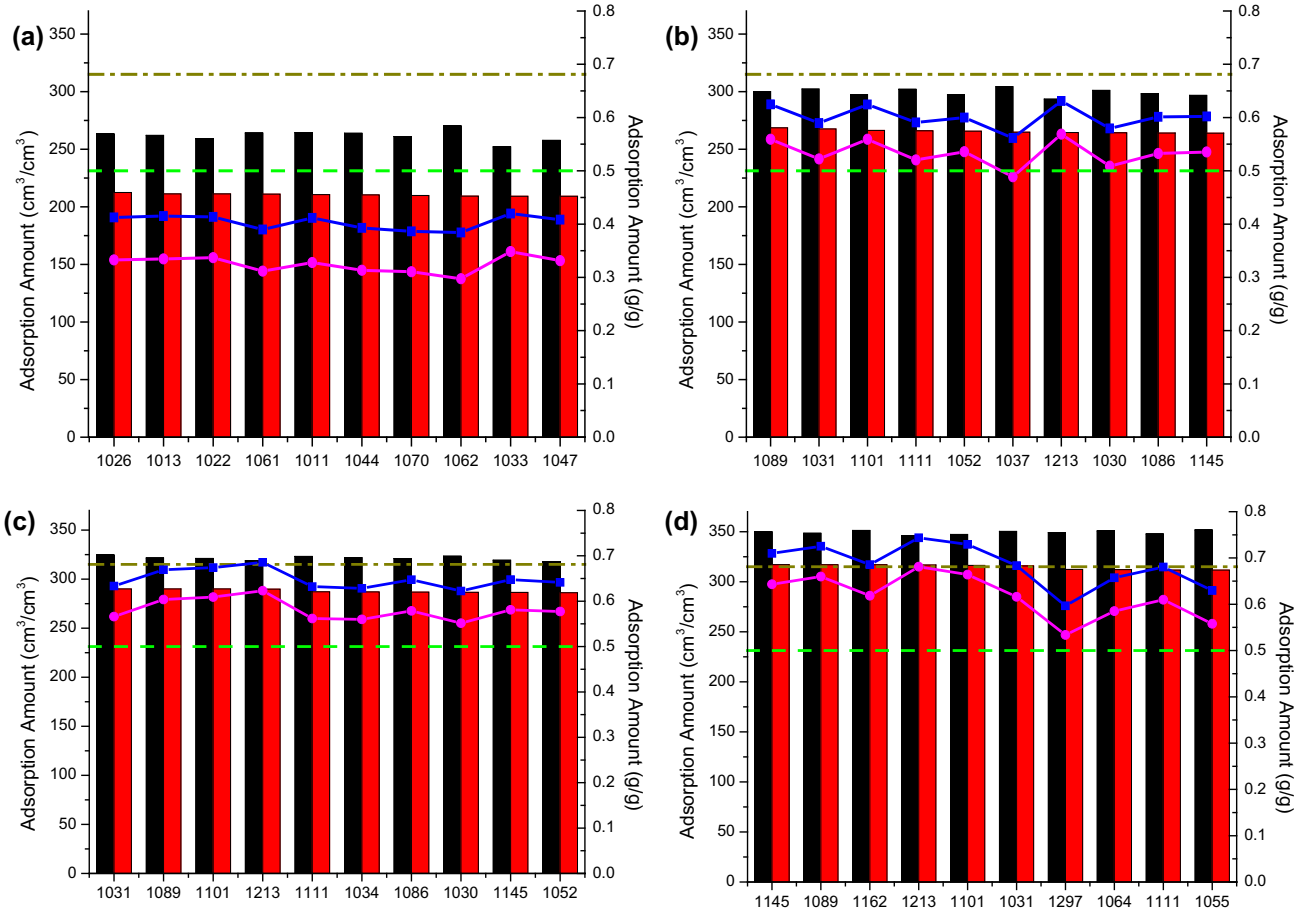

Fig. 2 Top ten MOF materials identified from simulation in terms of the volumetric delivery amount at 298 K and 5 bar. The themrodynamic condition at the stage of gas compression is: **a** 298 K and 70 bar; **b** 298 K and 170 bar; **c** 298 K and 250 bar; **d** 233 K and 75 bar. In each panel, the *dashed lines* correspond to the ARPA-E target for the volumetric delivery [315 cm^3(STP)/cm^3, *golden*] and for the weight delivery (0.5 g/g, *green*) (Color figure online)

shows the top 10 MOF candidates if the ARPA-E target is modified to the new compression temperature (233 K) and pressure (75 bar). We find that more than half of these materials could achieve the modified ARPA-E target in both volumetric and weight delivery categories. The reduction in compression temperature greatly improves the material performance for methane volumetric adsorption, much better than that at 298 K and 250 bar.

Table 1 lists the MOF candidates that yield the largest methane deliverable amount at various operational conditions (more data could be found in Tables S11-S30). We may attain the weight delivery target by either increasing the pressure or decreasing the temperature at the gas compression stage. However, the volumetric target cannot be reached solely by increasing the delivery temperature. Although none of the MOF materials we studied could meet the ARPA-E requirement at 298 K, over 90 % of the demand could be satisfied if we are allowed to increase the compression pressure to 170 bar and the release temperature to 358 K. We could further increase the volumetric delivery capacity by decreasing the gas compression temperature. For example, many MOF materials could achieve the ARPA-E target at a relatively low pressure (<50 bar) if the compression and delivery temperatures were set at 233 and 358 K, respectively. It is worth noting that temperature effect is also important for conventional gas storage such as CNG and LNG. For example, a gas tank contains 48 % more methane at 233 K and 250 bar than that of the same tank at 298 K and identical pressure. At lower pressure (e.g. compression at 35 bar and delivery at 5 bar), the net delivery amount of CNG increases 52 % at the reduced compression temperature 233 K. However, this amount is only about 17 % of its deliverable capacity at 298 K and 250 bar. By contrast, the same temperature change could increase over 75 % of the net methane delivery amount for MOFs, reaching more than 80 % of CNG deliverable capacity at 298 K and 250 bar.

The materials shown in Table 1 provide useful insights into future developments to meet the ARPA-E target for methane storage. These MOF candidates typically have a

Table 1 MOF materials with the maximum adsorption capacity in different categories

P[a]	Gas released at 298 K and 5 bar				Gas released at 358 K and 5 bar			
	ID	$\Gamma^{b}_{Del,V}$	ID	$\Gamma^{c}_{Del,M}$	ID	$\Gamma^{d}_{Del,V}$	ID	$\Gamma^{e}_{Del,M}$
35	1029	157	5003	0.29	1226	206	5003	0.32
70	1026	212	5001	0.59	1062	246	5001	0.61
100	1033	234	5001	0.79	1046	264	5001	0.81
150	1089	260	5077	1.08	1026	286	5077	1.09
170	1089	268	5077	1.19	1197	290	5077	1.21
200	1031	277	5124	1.34	1011	297	5124	1.35
250	1031	290	5124	1.52	1031	309	5124	1.53
35[f]	*1033*	*280*	*5003*	*0.64*	*1028*	*311*	*5003*	*0.67*
45[f]	*1026*	*291*	*5002*	*0.71*	*1028*	*321*	*5001*	*0.81*
75[f]	*1145*	*317*	*5007*	*1.16*	*1162*	*336*	*5007*	*1.18*

[a] Pressure in the units of bar at the compression stage

[b] $\Gamma_{del,V}$, the delivery amount in the units of cm^3/cm^3, if the gas is released at 298 K and 5 bar

[c] $\Gamma_{del,M}$, the delivery amount in the units of g/g

[d] $\Gamma_{del,V}$, the delivery amount, in the units of cm^3/cm^3, if the gas is released at 358 K and 5 bar

[e] $\Gamma_{del,M}$, the delivery amount in the units of g/g

[f] The compression temperature is set to 233 K (italic)

void fraction around 0.9 and specific surface area about 5000 m^2/g, with the building blocks containing large conjugated organic linkers and their derivatives with one or more alkane substitutions, incorporated with either zinc or copper oxides as the inorganic nodes. Figures S1 and S2 present the crystalline structures and the building blocks of these materials, and Tables 2 and 3 summarize, respectively, their pore characteristics and the simulation results for the isosteric heat of adsorption at different thermodynamic conditions. As discussed above, materials with high volumetric delivery amount approximately coincide those with large weight excess adsorption. Table 3 shows that these MOF materials have similar isosteric heat of adsorption at the compression stage, in the range of 14–16 kJ/mol regardless of the compression temperature. The results are similar if the gas release temperature is set to 358 K (Table S31), with slightly higher adsorption heat (15–19 kJ/mol) at the compression stage. Consistent with previously studies (Gomez-Gualdron et al. 2014; Rana et al. 2014), our simulation results indicate that a mild heat of adsorption (14–20 kJ/mol) is required for porous materials to achieve high volumetric deliverable amount.

We have also examined the characteristics of those MOF materials with the highest weight delivery amount. These MOF candidates are all in the category of high void fraction with zinc oxides as the inorganic nodes. In comparison to those MOFs with highest volumetric delivery amount, these materials have a much smaller isosteric heat of adsorption (7–9 kJ/mol). In addition, a higher compression pressure favors MOFs with larger void fraction but more gas interaction sites. The best MOF materials identified from the weight delivery amount typically have a very small density, with the volume surface area (m^2/cm^3) less than 15 % of the weight surface area (m^2/g). By contrast, the ratio is larger than 35 % for the MOFs with the highest volumetric delivery amount. Interestingly, the best MOF candidates identified by the weight delivery amount are relatively insensitive to the release temperature.

It is worth noting that molecular simulations are mostly based on perfect crystals while the MOF materials used in experiments and real applications typically appear as powders. Because of the void space between particles, realistic MOF materials have a much smaller overall density and thus lower volumetric gas storage capacity. To achieve higher volumetric surface area and thermal stability, we may minimize the void space between particles by pelletizing or other mechanical techniques (Dailly and Poirier 2011). For example, Purewal et al. processed MOF-5 powders into cylindrical tablets to increase the density up to 1.6 g/cm^3 by mechanical compaction, yielding a 350 % increase in volumetric H_2 adsorption with only 15 % loss in gravimetric storage capacity (Purewal et al. 2012). A similar procedure was used for Cu-BTC and UiO-66 with a substantial improvement of the gas adsorption capabilities (Bazer-Bachi et al. 2014).

4 Conclusions

In summary, we have investigated a large number of promising MOF materials and operational conditions that may be used to meet the ambitious ARPA-E target for methane storage. We propose that new materials development should be focused on improving the volumetric

Table 2 Characteristics of MOF materials listed in Table 1

	Void fr.	Dom. pore dia. (Å)	Max. pore dia. (Å)	Surf. area (m^2/g)	Surf. area (m^2/cm^3)	Dens. (cm^3/g)
1011	0.891	7.75	9.75	4940	2274	0.460
1026	0.885	7.75	10.25	4908	2243	0.457
1028	0.892	8.75	10.25	5109	2396	0.469
1029	0.892	7.75	10.25	5030	2414	0.480
1031	0.917	10.25	12.25	5526	2028	0.367
1033	0.897	8.75	10.25	5067	2178	0.430
1046	0.872	7.75	9.75	4723	2328	0.493
1062	0.868	7.75	9.75	4623	2332	0.504
1089	0.916	11.25	13.25	5435	1870	0.344
1145	0.898	12.75	13.75	5332	1884	0.353
1162	0.880	11.25	12.75	5862	2153	0.367
1197	0.865	7.75	12.25	4558	2094	0.460
1226	0.871	7.75	9.75	3513	2137	0.608
5001	0.967	20.75	24.75	5746	777	0.135
5002	0.966	24.25	24.75	5622	859	0.153
5003	0.966	24.75	24.75	5550	872	0.157
5007	0.961	24.25	24.75	5743	776	0.135
5077	0.952	24.75	24.75	6396	763	0.119
5124	0.949	23.25	24.75	6340	751	0.118

Table 3 Isosteric heat of adsorption (Qst) for the MOF materials listed in Table 1 at different themrodynamic conditions

P[a]	ID	Qst[b] (kJ/mol)	Qst^{c}_{5bar} (kJ/mol)	ID	Qst[b] (kJ/mol)	Qst^{c}_{5bar} (kJ/mol)
35	1029	15.84	*13.09*	5003	8.30	*9.62*
70	1026	16.29	*12.59*	5001	7.30	*8.17*
100	1033	15.07	*11.83*	5001	7.42	*8.17*
150	1089	13.84	*11.44*	5077	7.30	*6.39*
170	1089	13.59	*11.44*	5077	7.55	*6.39*
200	1031	14.70	*11.50*	5124	7.96	*6.74*
250	1031	15.02	*11.50*	5124	8.68	*6.74*
35	1033	**16.11**[d]	*11.83*	5003	**8.37**[d]	*9.62*
45	1026	**17.25**[d]	*12.59*	5002	**8.28**[d]	*9.22*
75	1145	**15.43**[d]	*11.78*	5007	**8.16**[d]	*8.18*

[a] Pressure in units of bar at the compression stage

[b] Compression temperature at 298 K

[c] Gas release at 5 bar and 298 K (italic)

[d] Gas compression at 233 K (bold)

delivery amount rather than the gravimetric gas storage capacity or other criteria that are often quoted in the literature. While none of MOF materials known today meet the original ARPA-E standards, the top ranked MOF is able to deliver over 90 % of the required methane amount if methane is compressed at 298 K and 170 bar and released at 358 K and 5 bar. A large number of MOF materials could reach the ARPA-E target if the compression temperature is set at 233 K. A further analysis of these materials indicates that the promising MOFs should have large conjugated phenyl ring structure as organic linker and copper oxide as inorganic node, concomitant with a void fraction around 0.9, specific surface area around 5000 m^2/g, and a moderate isosteric heat of adsorption (14–20 kJ/mol).

Acknowledgments The project is financially supported by the COR Research Fellowship from the University of California at Riverside.

References

ARPA-E. 2015. MOVE Program Overview. http://arpa-e.energy.gov

BASF. BASF-MOF. http://www.catalysts.basf.com/

Bazer-Bachi, D., Assié, L., Lecocq, V., Harbuzaru, B., Falk, V.: Towards industrial use of metal-organic framework: impact of shaping on the MOF properties. Powder Technol. **255**, 52–59 (2014)

Celzard, A., Fierro, V.: Preparing a suitable material designed for methane storage: a comprehensive report. Energy Fuels **19**, 573–583 (2005)

Chui, S.S.Y., Lo, S.M.F., Charmant, J.P.H., Orpen, A.G., Williams, I.D.: A chemically functionalizable nanoporous material $[Cu_3(TMA)_2(H_2O)_3]_n$. Science **283**, 1148–1150 (1999)

Dailly, A., Poirier, E.: Evaluation of an industrial pilot scale densified MOF-177 adsorbent as an on-board hydrogen storage medium. Energy Environ. Sci. **4**, 3527–3534 (2011)

Düren, T., Sarkisov, L., Yaghi, O.M., Snurr, R.Q.: Design of new materials for methane storage. Langmuir **20**, 2683–2689 (2004)

Eddaoudi, M., Kim, J., Rosi, N., Vodak, D., Wachter, J., O'Keeffe, M., Yaghi, O.M.: Systematic design of pore size and functionality in isoreticular MOFs and their application in methane storage. Science **295**, 469–472 (2002a)

Eddaoudi, M., Kim, J., Vodak, D., Sudik, A., Wachter, J., O'Keeffe, M., Yaghi, O.M.: Geometric requirements and examples of important structures in the assembly of square building blocks. Proc. Natl. Acad. Sci. USA. **99**, 4900–4904 (2002b)

Eddaoudi, M., Moler, D.B., Li, H., Chen, B., Reineke, T.M., O'keeffe, M., Yaghi, O.M.: Modular chemistry: secondary building units as a basis for the design of highly porous and robust metal-organic carboxylate frameworks. Acc. Chem. Res. **34**, 319–330 (2001)

Frenkel, D., Smit, B.: Understanding Molecular Simulation: From Algorithms to Applications. Academic Press, San Diego (2001)

Frost, H., Duren, T., Snurr, R.Q.: Effects of surface area, free volume, and heat of adsorption on hydrogen uptake in metal-organic frameworks. J. Phys. Chem. B **110**, 9565–9570 (2006)

Fu, J., Liu, Y., Tian, Y., Wu, J.: Density functional methods for fast screening of metal-organic frameworks for hydrogen storage. J. Phys. Chem. C **119**, 5374–5385 (2015)

Gómez-Gualdrón, D.A., Wilmer, C.E., Farha, O.K., Hupp, J.T., Snurr, R.Q.: Exploring the limits of methane storage and delivery in nanoporous materials. J. Phys. Chem. C **118**, 6941–6951 (2014)

Gándara, F., Furukawa, H., Lee, S., Yaghi, O.M.: High methane storage capacity in aluminum metal-organic frameworks. J. Am. Chem. Soc. **136**, 5271–5274 (2014)

Garberoglio, G., Skoulidas, A.I., Johnson, J.K.: Adsorption of gases in metal organic materials: comparison of simulations and experiments. J. Phys. Chem. B **109**, 13094–13103 (2005)

Gomez-Gualdron, D.A., Gutov, O.V., Krungleviciute, V., Borah, B., Mondloch, J.E., Hupp, J.T., Yildirim, T., Farha, O.K., Snurr, R.Q.: Computational design of metal-organic frameworks based on stable zirconium building units for storage and delivery of methane. Chem. Mater. **26**, 5632–5639 (2014)

Guo, Z., Wu, H., Srinivas, G., Zhou, Y., Xiang, S., Chen, Z., Yang, Y., Zhou, W., O'Keeffe, M., Chen, B.: A Metal-organic framework with optimized open metal sites and pore spaces for high methane storage at room temperature. Angew. Chem. Int. Ed. **50**, 3178–3181 (2011)

He, Y., Zhou, W., Qian, G., Chen, B.: Methane storage in metal-organic frameworks. Chem. Soc. Rev. **43**, 5657–5678 (2014)

Johnson, J.K., Zollweg, J.A., Gubbins, K.E.: The Lennard-Jones equation of state revisited. Mol. Phys. **78**, 591–618 (1993)

Li, B., Wen, H.-M., Wang, H., Wu, H., Tyagi, M., Yildirim, T., Zhou, W., Chen, B.: A porous metal-organic framework with dynamic pyrimidine groups exhibiting record high methane storage working capacity. J. Am. Chem. Soc. **136**, 6207–6210 (2014a)

Li, B., Wen, H.M., Zhou, W., Chen, B.L.: Porous metal-organic frameworks for gas storage and separation: what, how, and why? J. Phys. Chem. Lett. **5**, 3468–3479 (2014b)

Liu, B., Smit, B.: Molecular simulation studies of separation of CO_2/N_2, CO_2/CH_4, and CH_4/N_2 by ZIFs. J. Phys. Chem. C **114**, 8515–8522 (2010)

Liu, J., Thallapally, P.K., McGrail, B.P., Brown, D.R., Liu, J.: Progress in adsorption-based CO_2 capture by metal-organic frameworks. Chem. Soc. Rev. **41**, 2308–2322 (2012)

Lozano-Castelló, D., Alcañiz-Monge, J., de la Casa-Lillo, M.A., Cazorla-Amorós, D., Linares-Solano, A.: Advances in the study of methane storage in porous carbonaceous materials. Fuel **81**, 1777–1803 (2002)

Ma, S., Sun, D., Simmons, J.M., Collier, C.D., Yuan, D., Zhou, H.-C.: Metal-organic framework from an anthracene derivative containing nanoscopic cages exhibiting high methane uptake. J. Am. Chem. Soc. **130**, 1012–1016 (2007)

Ma, S., Sun, D., Simmons, J.M., Collier, C.D., Yuan, D., Zhou, H.C.: Metal-organic framework from an anthracene derivative containing nanoscopic cages exhibiting high methane uptake. J. Am. Chem. Soc. **130**, 1012–1016 (2008)

Makal, T.A., Li, J.-R., Lu, W., Zhou, H.-C.: Methane storage in advanced porous materials. Chem. Soc. Rev. **41**, 7761–7779 (2012)

Martin, M.G., 2013. MCCCS Towhee, http://towhee.sourceforge.net

Martin, M.G., Siepmann, J.I.: Transferable potentials for phase equilibria. 1. United-atom description of n-alkanes. J. Phys. Chem. B **102**, 2569–2577 (1998)

Martin, R.L., Simon, C.M., Smit, B., Haranczyk, M.: In silico design of porous polymer networks: high-throughput screening for methane storage materials. J. Am. Chem. Soc. **136**, 5006–5022 (2014)

Mason, J.A., Veenstra, M., Long, J.R.: Evaluating metal-organic frameworks for natural gas storage. Chem. Sci. **5**, 32–51 (2014)

Peng, Y., Krungleviciute, V., Eryazici, I., Hupp, J.T., Farha, O.K., Yildirim, T.: Methane storage in metal-organic frameworks: current records, surprise findings, and challenges. J. Am. Chem. Soc. **135**, 11887–11894 (2013a)

Peng, Y., Srinivas, G., Wilmer, C.E., Eryazici, I., Snurr, R.Q., Hupp, J.T., Yildirim, T., Farha, O.K.: Simultaneously high gravimetric and volumetric methane uptake characteristics of the metal–organic framework NU-111. Chem. Commun. **49**, 2992–2994 (2013b)

Purewal, J.J., Liu, D., Yang, J., Sudik, A., Siegel, D.J., Maurer, S., Müller, U.: Increased volumetric hydrogen uptake of MOF-5 by powder densification. Int. J. Hydrog. Energy **37**, 2723–2727 (2012)

Rana, M.K., Koh, H.S., Zuberi, H., Siegel, D.J.: Methane storage in metal-substituted metal-organic frameworks: thermodynamics, usable capacity, and the impact of enhanced binding sites. J. Phys. Chem. C **118**, 2929–2942 (2014)

Rappe, A.K., Casewit, C.J., Colwell, K.S., Goddard, W.A., Skiff, W.M.: Uff, a full periodic-table force-field for molecular mechanics and molecular-dynamics simulations. J. Am. Chem. Soc. **114**, 10024–10035 (1992)

Rosi, N.L., Eckert, J., Eddaoudi, M., Vodak, D.T., Kim, J., O'Keeffe, M., Yaghi, O.M.: Hydrogen storage in microporous metal-organic frameworks. Science **300**, 1127–1129 (2003)

Skoulidas, A.I., Sholl, D.S.: Self-diffusion and transport diffusion of light gases in metal-organic framework materials assessed using molecular dynamics simulations. J. Phys. Chem. B **109**, 15760–15768 (2005)

Suh, M.P., Park, H.J., Prasad, T.K., Lim, D.-W.: Hydrogen storage in metal-organic frameworks. Chem. Rev. **112**, 782–835 (2011)

Sumida, K., Rogow, D.L., Mason, J.A., McDonald, T.M., Bloch, E.D., Herm, Z.R., Bae, T.-H., Long, J.R.: Carbon dioxide capture in metal-organic frameworks. Chem. Rev. **112**, 724–781 (2011)

Walton, K.S., Snurr, R.Q.: Applicability of the BET method for determining surface areas of microporous metal-organic frameworks. J. Am. Chem. Soc. **129**, 8552–8556 (2007)

Wilmer, C.E., Farha, O.K., Yildirim, T., Eryazici, I., Krungleviciute, V., Sarjeant, A.A., Snurr, R.Q., Hupp, J.T.: Gram-scale, high-yield synthesis of a robust metal–organic framework for storing methane and other gases. Energy Environ. Sci. **6**, 1158–1163 (2013)

Wilmer, C.E., Leaf, M., Lee, C.Y., Farha, O.K., Hauser, B.G., Hupp, J.T., Snurr, R.Q.: Large-scale screening of hypothetical metal–organic frameworks. Nat. Chem. **4**, 83–89 (2012)

Wu, H., Zhou, W., Yildirim, T.: High-capacity methane storage in metal–organic frameworks M2 (dhtp): the important role of open metal sites. J. Am. Chem. Soc. **131**, 4995–5000 (2009)

Yaghi, O.M., O'Keeffe, M., Ockwig, N.W., Chae, H.K., Eddaoudi, M., Kim, J.: Reticular synthesis and the design of new materials. Nature **423**, 705–714 (2003)

Yang, Q., Zhong, C.: Molecular simulation of carbon dioxide/methane/hydrogen mixture adsorption in metal-organic frameworks. J. Phys. Chem. B **110**, 17776–17783 (2006)